

# On the Mixing of Diffusing Particles

E. Ben-Naim

*Theoretical Division and Center for Nonlinear Studies,  
Los Alamos National Laboratory, Los Alamos, New Mexico 87545*

We study how the order of  $N$  independent random walks in one dimension evolves with time. Our focus is statistical properties of the inversion number  $m$ , defined as the number of pairs that are out of sort with respect to the initial configuration. In the steady-state, the distribution of the inversion number is Gaussian with the average  $\langle m \rangle \simeq N^2/4$  and the standard deviation  $\sigma \simeq N^{3/2}/6$ . The survival probability,  $S_m(t)$ , which measures the likelihood that the inversion number remains below  $m$  until time  $t$ , decays algebraically in the long-time limit,  $S_m \sim t^{-\beta_m}$ . Interestingly, there is a spectrum of  $N(N-1)/2$  distinct exponents  $\beta_m(N)$ . We also find that the kinetics of first-passage in a circular cone provides a good approximation for these exponents. When  $N$  is large, the first-passage exponents are a universal function of a single scaling variable,  $\beta_m(N) \rightarrow \beta(z)$  with  $z = (m - \langle m \rangle)/\sigma$ . In the cone approximation, the scaling function is a root of a transcendental equation involving the parabolic cylinder equation,  $D_{2\beta}(-z) = 0$ , and surprisingly, numerical simulations show this prediction to be exact.

PACS numbers: 05.40.Fb, 02.50.Cw, 02.30.Ey, 05.40.-a

## I. INTRODUCTION

Consider the permutation 3142 of the four elements  $\{1, 2, 3, 4\}$ . Three pairs:  $(1, 3)$ ,  $(2, 3)$ , and  $(2, 4)$  are inverted in this permutation. The inversion number, defined as the total number of pairs that are out of sort, provides a natural measure for how “scrambled” a list of elements is. This basic combinatorial quantity [1–4] is helpful in many contexts. In computer science, the inversion number plays an important role in sorting and ranking algorithms [5]. Common on the web (“customers who like ... may also like ...”), recommendations for books, songs, and movies use inversions to quantify how close the preferences of two customers are [6].

The number of inversions can also be used to measure how the order of a group of particles in one dimension changes with time. Figure 1 illustrates a space-time diagram of four diffusing particles. The number of inversions changes whenever two trajectories cross. Depending on the initial order of the two respective particles, a crossing may either introduce a new inversion or undo an existing one. Consequently, the inversion number either increases or decreases by one. Therefore, the inversion number equals the difference between the number of crossings of the first kind and the number of crossings of the second kind.

Mixing dynamics has been extensively studied in the context of fluids [7, 8] and granular materials [9], but much less attention has been given to mixing in the context of diffusion [10, 11]. In this study, we consider an ensemble of  $N$  diffusing particles in one-dimension, a system that is widely used to model the transport of colloidal and biological particles in narrow channels [12, 13]. We use the inversion number to measure the degree to which particles mix. Clearly, a persistent small inversion number indicates a poorly mixed system, while a large inversion number implies that the opposite is true.

We first study how the distribution of the inversion

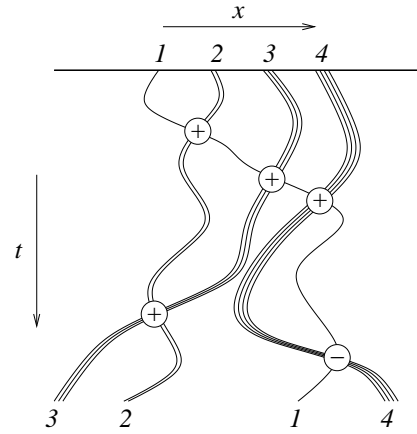


FIG. 1: Space-time diagram of a four-particle system. The circled +s and -s indicate whether the inversion number increases or decreases when two trajectories cross. Four out of the five crossings increase the inversion number, and accordingly, the inversion number increases from  $m = 0$  to  $m = 3$ .

number evolves with time. We find that there is a transient regime in which the average inversion number as well as the standard deviation in this quantity both grow as the square-root of time. The distribution of the inversion number is stationary beyond this transient regime. When the number of particles is sufficiently large, the probability distribution function is always Gaussian, whether in the transient regime or in the steady-state.

Our main focus is first-passage properties [14] of the inversion number. We ask: what is  $S_m(t)$ , the probability that the inversion number remains smaller than  $m$  up to time  $t$ . For small values of  $m$ , the survival probability  $S_m$  measures the likelihood that the particles remain poorly mixed throughout the evolution. Generally, the probabilities  $S_m$  decay as a power law at large times,  $S_m \sim t^{-\beta_m}$ . In general, there is a broad spectrum of

$N(N-1)/2$  distinct exponents,  $\{\beta_1, \beta_2, \dots, \beta_{N(N-1)/2}\}$ , that governs the asymptotic decay of the survival probabilities.

We heavily use first-passage kinetics of a single particle that diffuses inside a circular cone [15–17] to understand the asymptotic behavior of  $S_m$ . We first utilize two-dimensional cones to obtain the first-passage exponents for a three-particle system exactly. Furthermore, we employ circular cones in  $N-1$  dimensions and find good approximate values for the first-passage exponents.

The cone approximation correctly predicts that when the number of particles is large, the exponents become a universal function,  $\beta_m(N) \rightarrow \beta(z)$ , of the scaling variable  $z = (m - \langle m \rangle)/\sigma$ . Here,  $\langle m \rangle$  and  $\sigma$  are the average and standard deviation of the distribution of inversion number, at the steady-state. Interestingly, our numerical simulations show that the cone approximation yields the exact scaling function  $\beta(z)$  as a root of a transcendental equation involving the parabolic cylinder function.

The rest of this paper is organized as follows. In section II, we introduce our basic system and define the inversion number. Stationary and transient properties of the distribution of the inversion number are discussed in sections III and IV, respectively. In section V, we use the cone approximation to understand first-passage properties of the inversion number. Scaling and extremal properties of the first-passage exponents are the focus of section VI. We conclude in section VII.

## II. THE INVERSION NUMBER

Our goal is to characterize how the order of an ensemble of diffusing particles changes with time. We conveniently use an ordinary random walk [18–20] to model the trajectory of a diffusing particle [21]. Our system includes  $N$  identical particles that move on an unbounded one-dimensional lattice. The particles are completely independent: at each step one particle is selected at random and it moves, with an equal probability, either to the left,  $x \rightarrow x-1$ , or to the right,  $x \rightarrow x+1$ . After each elementary step, time is augmented by the inverse number of particles,  $t \rightarrow t+1/N$ , so that each particle moves once per unit time.

We index the particles according to their initial position with the leftmost particle labeled  $n=1$  and the rightmost particle labeled  $n=N$  (Figure 1). Let  $x_n(t)$  be the position of the  $n$ th particle at time  $t$ . By definition,

$$x_1(0) < x_2(0) < \dots < x_{N-1}(0) < x_N(0), \quad (1)$$

but the initial order unravels with time. Consider, for example, the four-particle system illustrated in Figure 1. The particles reach a state where  $x_3 < x_2 < x_1 < x_4$  with three pairs, (1, 2), (1, 3), and (2, 3) being out of sort compared with time  $t=0$ . In general, a pair of particles for which  $x_i(t) > x_j(t)$  and  $i < j$  constitutes an inversion.

Formally, the total number of inversions,  $m$ , is given by

$$m(t) = \sum_{i=1}^N \sum_{j=i+1}^N \Theta(x_i(t) - x_j(t)). \quad (2)$$

Here,  $\Theta(x)$  is the Heaviside step function:  $\Theta(x) = 1$  for  $x > 0$  and  $\Theta(x) = 0$  for  $x \leq 0$ . The total number of pairs is  $M = \binom{N}{2}$ , and hence, the variable  $m$  is within the bounds  $0 \leq m \leq M$  with

$$M = \frac{N(N-1)}{2}. \quad (3)$$

The inversion number is minimal,  $m=0$ , when the order is exactly the same as in the initial configuration, and it is maximal,  $m=M$ , when the order is the mirror image of the initial state.

The inversion number changes whenever two trajectories cross (Figure 1). A crossing either adds a new inversion or removes an existing one. Thus, we may assign a positive or a negative “charge” to each crossing as illustrated in Figure 1. The inversion number,  $m(t)$ , is simply the sum of all of the charges up to time  $t$ .

## III. THE MAHONIAN DISTRIBUTION

We first discuss basic statistical characteristics of the inversion number including the average, the variance, and more generally, the probability distribution function. At large time  $t$ , each random walk explores a region of size  $\sqrt{t}$ , and the probability of finding the particle at any lattice site inside this region is effectively uniform. This simple fact already implies that memory of the initial position fades with time. We thus expect that after sufficient time elapses, there is no memory of the initial order, and the order of the particles is completely random.

To understand statistics of the inversion number for randomly ordered particles we consider the set of all  $N!$  permutations of the  $N$  elements  $\{1, 2, \dots, N\}$ . In the random state, each permutation of these elements occurs with probability  $1/N!$ . The probability  $P_m(N)$  that the inversion number equals  $m$  for a random permutation is well known as the Mahonian distribution in probability theory [1, 2, 5]. We highlight key features of this probability distribution as it plays a central role in our study.

Let  $Q_m(N) = N!P_m(N)$  be the number of permutations of  $N$  elements with exactly  $m$  inversions. For example, when  $N=3$ , one permutation (123) is free of inversions, there are two permutations with one inversion (213, 132), two permutations with two inversions (312, 231), and a single permutation with three inversions (321). Hence,  $Q_0(3) = Q_3(3) = 1$  while  $Q_1(3) = Q_2(3) = 2$ . We list the distribution of the inversion number for  $N \leq 4$ ,

$$(P_0, P_1, \dots, P_M) = \frac{1}{N!} \times \begin{cases} (1) & N=1, \\ (1, 1) & N=2, \\ (1, 2, 2, 1) & N=3, \\ (1, 3, 5, 6, 5, 3, 1) & N=4. \end{cases}$$

Of course,  $P_m(N)$  is nonzero if and only if  $0 \leq m \leq M$ .

Since the mirror image of a configuration with  $m$  inversions necessarily has  $M - m$  inversions, the probability distribution satisfies  $P_m = P_{M-m}$ . Hence, the distribution is symmetric about  $m = M/2$ , and the average  $\langle m \rangle \equiv \sum_m m P_m$  is simply

$$\langle m \rangle = \frac{N(N-1)}{4}. \quad (4)$$

Therefore, the average grows quadratically with the total number of particles when  $N \gg 1$ .

The Mahonian distribution satisfies the simple recursion relation

$$P_m(N) = \frac{1}{N} \sum_{l=0}^{N-1} P_{m-l}(N-1), \quad (5)$$

with  $P_m(1) = \delta_{m,0}$ . This recursion reflects that every permutation of  $N$  elements can be generated from a permutation of  $N-1$  elements by inserting the  $N$ th element in any of the  $N$  possible positions. Depending on where this last element is added, the number of inversions increases by an amount  $\Delta m = 0, 1, \dots, N-1$ .

Let us now introduce the generating function,

$$\mathcal{P}(s, N) = \sum_{m=0}^M P_m(N) s^m. \quad (6)$$

For instance,  $\mathcal{P}(s, 1) = 1$ ,  $\mathcal{P}(s, 2) = (1+s)/2!$  and  $\mathcal{P}(s, 3) = (1+s)(1+s+s^2)/3!$ . In general, the generating function is given by the product [5]

$$\mathcal{P}(s, N) = \frac{1}{N!} \prod_{n=1}^N (1 + s + s^2 + \dots + s^{n-1}), \quad (7)$$

as also follows from the recursion (5).

We can confirm the average (4) by differentiating the generating function once,  $\mathcal{P}'(s=1) = \langle m \rangle$ , where the prime represents differentiation with respect  $s$ . By differentiating the generating function twice and using  $\mathcal{P}''(s=1) = \langle m(m-1) \rangle$ , we obtain the variance [5],  $\sigma^2 = \langle m^2 \rangle - \langle m \rangle^2$ ,

$$\sigma^2 = \frac{N(N-1)(2N+5)}{72}. \quad (8)$$

This expression is obtained from  $\sigma^2 = \sum_{l=1}^N \frac{l^2-1}{12}$ . Therefore, the standard deviation is rather large,  $\sigma \simeq N^{3/2}/6$ , when  $N \gg 1$ .

The mean (4) and the variance (8) fully specify the probability distribution function for an asymptotically large number of particles. The Mahonian distribution becomes a function of a single variable,  $P_m(N) \rightarrow \Phi(z)$ , with the scaling variable

$$z = \frac{m - \langle m \rangle}{\sigma}. \quad (9)$$

The probability distribution function,  $\Phi(z)$ , is normal, that is, a Gaussian with zero mean and unit variance [2, 22],

$$\Phi(z) \simeq \frac{1}{\sqrt{2\pi}} \exp\left(-\frac{z^2}{2}\right). \quad (10)$$

To see that the central limit theorem applies, we convert the generating function into a Fourier transform, and then show that the Fourier transform is Gaussian in the large- $N$  limit [23].

The variable  $z$  is a more transparent measure in the following sense. A value of  $z$  of order one implies fairly random order. Indeed, according to the normal distribution (10), the inversion number falls within three standard deviations from the mean,  $|z| < 3$ , with probability 0.997. A large value,  $|z| \gg 1$ , indicates that the particle order strongly resembles the initial configuration (if  $z > 0$ ) or its mirror image (if  $z < 0$ ).

#### IV. TRANSIENT BEHAVIOR

By definition, the inversion number is zero initially,  $m(0) = 0$ . At least partially, the initial order is preserved in the early stages of evolution, and the number of inversions must be substantially lower than (4).

We consider the natural initial condition where the particles occupy  $N$  consecutive lattice sites:  $x_i(0) = i$ , for all  $i = 1, 2, \dots, N$ . Early on, particles “interact” only within their local neighborhood. The interaction length,  $\ell$ , grows diffusively with time,  $\ell \sim \sqrt{t}$ . On this length scale, particles are well-mixed, and according to (4), the number of inversions *per particle* is proportional to the number of interacting particles,  $\ell$ . Hence, the average number of inversions grows according to  $\langle m(t) \rangle \sim N\ell \sim N\sqrt{t}$ . As a consequence,

$$\langle m(t) \rangle \simeq \begin{cases} \text{const.} \times N\sqrt{t} & 1 \ll t \ll N^2, \\ N^2/4 & N^2 \ll t, \end{cases} \quad (11)$$

when  $N \gg 1$ . The two expressions match at  $t \sim N^2$ , a diffusive time scale that can be viewed as the mixing time. Therefore, there is a transient regime in which the inversion number grows as the square-root of time, followed by a steady-state, in which the average is given by (4).

We obtain the variance using a similar heuristic argument. According to (8), the variance per particle is quadratic in the number of interacting particles,  $\sigma^2 \sim N\ell^2$ . Therefore,  $\sigma^2 \sim Nt$  in the transient regime,

$$\sigma(t) \simeq \begin{cases} \text{const} \times \sqrt{Nt} & 1 \ll t \ll N^2, \\ N^{3/2}/6 & N^2 \ll t. \end{cases} \quad (12)$$

As expected, the transient behavior matches the steady-state behavior (8) at the diffusive time scale  $t \sim N^2$ . Like the average, the standard deviation also grows as the square root of time.

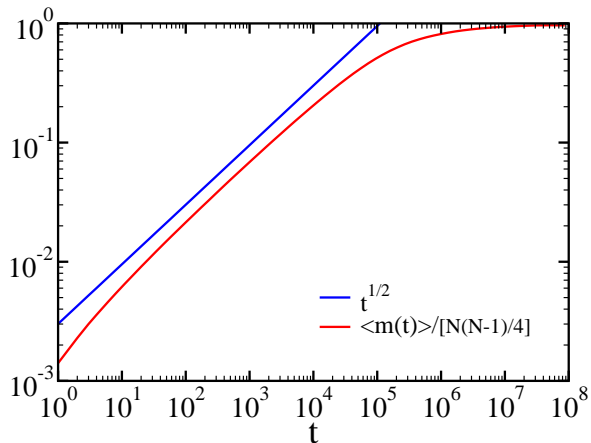


FIG. 2: The normalized average  $\langle m(t) \rangle / [N(N-1)/4]$  versus time  $t$ . The results correspond to an average over  $10^2$  independent realizations of a system with  $N = 10^3$  random walks. Also shown for reference is a line with slope  $1/2$ .

As shown in Figure 2, results of numerical simulations confirm the scaling behavior (11). Moreover, the numerically measured average matches the steady-state value corresponding to the Mahonian distribution. We also verified that the stationary distribution is Gaussian with the variance (8).

The simulations also show that the time-dependent distribution of inversion number,  $p_m(N, t)$ , is Gaussian throughout the transient regime (Figure 3):

$$p_m(N, t) \simeq \frac{1}{\sqrt{2\pi\sigma^2(t)}} \exp\left[-\frac{(m - \langle m(t) \rangle)^2}{2\sigma^2(t)}\right]. \quad (13)$$

This behavior provides further support for our heuristic argument. Indeed, if the particles are well-mixed locally, then the distribution of the number of inversions per particle is Gaussian, and as the sum of  $N$  Gaussian variables, the total inversion number must also have a Gaussian distribution.

We used two different algorithms to simulate the diffusion process. In the naive algorithm, we randomly select a particle and move it to a randomly-chosen neighboring site. We increase time by  $1/N$  after each jump. To calculate the inversion number, we use the formula (2), but since this enumeration requires  $\mathcal{O}(N^2)$  operations, this simulation method is inefficient at large  $N$ .

To overcome this difficulty, we introduced a variant where each lattice site may be occupied by at most one particle. At each step we pick one particle at random and attempt to move it by one site. This move is always accepted if the neighboring site is vacant, but otherwise, it is accepted with probability  $1/2$ . In the latter case, we merely exchange the identities of the respective particles, and as appropriate, update the inversion number by either  $+1$  or  $-1$ . In our implementation, there are two arrays: the first lists the particle positions, *in order*, and the second lists the original position of each particle in the first list. This algorithm has a fixed computational

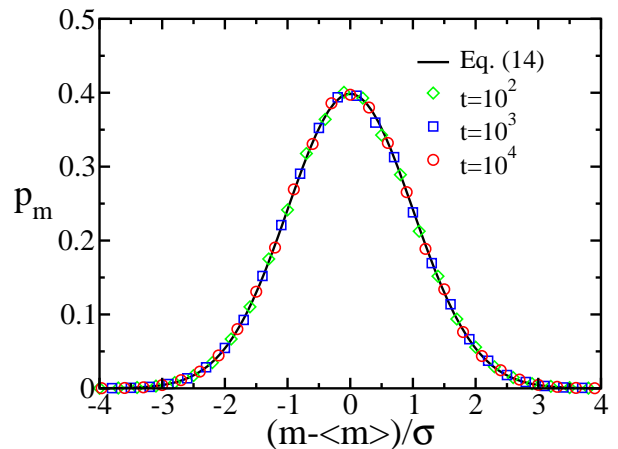


FIG. 3: The distribution of the inversion number in the intermediate time regime  $1 \ll t \ll N^2$ . Shown is the distribution  $p_m \equiv p_m(N, t)$  versus the variable  $(m - \langle m(t) \rangle) / \sigma(t)$ . The results are from  $10^5$  independent realizations of a system with  $N = 10^3$  random walks. The distribution is shown at times  $t = 10^2$  (diamonds),  $t = 10^3$  (squares), and  $t = 10^4$  (circles). Also shown for reference is the normal distribution (13).

cost per step, and it automatically keeps track of the inversion number. We rely on the fact that in one dimension, noninteracting random walks are equivalent to random walks that interact by exclusion [24–27]. Still, we verified that the two algorithms yield essentially the same results. We utilized the naive algorithm to simulate small systems with  $N < 10$ , but otherwise, we used the efficient algorithm.

## V. FIRST-PASSAGE KINETICS

We have seen that the inversion number, which grows quadratically with the number of particles, can be quite large. Yet, if the mixing is poor and the particle trajectories rarely cross, the inversion number remains small. To quantify how common such a scenario is, we study first-passage kinetics [14, 28]. In particular, we ask: what is the probability,  $S_m(t)$ , that the inversion number remains smaller than  $m$  until time  $t$ . This “survival” probability is closely related to the first-passage probability as  $[-dS_m/dt] \times dt$  is the probability that the inversion number reaches  $m$  for the first time during the infinitesimal time interval  $(t, t + dt)$ .

The quantity  $S_1$  is the probability that the original order is perfectly maintained, or equivalently, the likelihood that none of the trajectories cross. This survival probability decays as a power law, with a rather large exponent,

$$S_1 \sim t^{-N(N-1)/4}, \quad (14)$$

in the long-time limit [29–34]. Our goal is to understand how this asymptotic behavior changes as the threshold  $m$  increases.

When  $N = 2$ , the separation between the two random walks itself undergoes a random walk. Hence,  $S_1$  is equivalent to the survival probability of a one-dimensional random walk in the vicinity of a trap, and  $S_1 \sim t^{-1/2}$  in agreement with (14).

When  $N = 3$ , we conveniently map the three random walks onto a single ‘‘compound’’ random walk in three dimensions with the coordinates  $(x_1, x_2, x_3)$ . To find  $S_1$ , we require that the compound walk remains inside the region  $x_1 < x_2 < x_3$ . We may view the boundary of this region as absorbing, and then,  $S_1(t)$  equals the likelihood that the compound walk survives at time  $t$ . The absorbing boundary forms a wedge because it is defined by the intersection of two planes,  $x_1 = x_2$  and  $x_2 = x_3$ . Generally, the survival probability of a particle that diffuses inside an absorbing wedge decays algebraically,

$$S \sim t^{-1/(4V)}, \quad (15)$$

where  $V = \alpha/\pi$  is the normalized opening angle [35]. (The opening angle  $0 < \alpha \leq \pi$  is the angle between the wedge axis and the wedge boundary.) Alternatively,  $0 < V \leq 1$  is the fraction of the total solid angle enclosed by the wedge. The region  $x_1 < x_2 < x_3$  occupies a fraction  $V_1 = \frac{1}{3!} = \frac{1}{6}$  of space and hence,  $S_1 \sim t^{-3/2}$ , as also follows from (14). To find  $S_2$  and  $S_3$ , we note that the regions in which the compound walk is allowed to move are always wedges (the three planes  $x_1 = x_2$ ,  $x_1 = x_3$ , and  $x_2 = x_3$  divide space into six equal wedges [36].) Moreover, the fraction of total solid angle enclosed by the absorbing boundaries is given by the cumulative distribution of inversion number:  $V_2 = \frac{1}{3!} + \frac{2}{3!} = \frac{1}{2}$  and  $V_3 = \frac{1}{3!} + \frac{2}{3!} + \frac{2}{3!} = \frac{5}{6}$ . Hence, all three survival probabilities decay algebraically with time [14],

$$S_1 \sim t^{-3/2}, \quad S_2 \sim t^{-1/2}, \quad S_3 \sim t^{-3/10}, \quad (16)$$

and there are three distinct first-passage exponents.

The asymptotic behaviors (16) suggest that all of the survival probabilities decay algebraically,

$$S_m \sim t^{-\beta_m}, \quad (17)$$

in the long-time limit. Moreover, there is a large family of exponents

$$\beta_1 > \beta_2 > \dots > \beta_{N(N-1)/2}, \quad (18)$$

that characterizes the power-law decay (17). We stress that the exponents depend on two variables, the threshold  $m$  and the number of particles  $N$ ,  $\beta \equiv \beta_m(N)$ . We already know the exact values  $\beta_1(3) = 3/2$ ,  $\beta_2(3) = 1/2$ , and  $\beta_3(3) = 3/10$  as well as  $\beta_1(N) = N(N-1)/4$ .

Our numerical simulations confirm that indeed, there is a large spectrum of exponents. As shown in Figure 4, there are six decay exponents when  $N = 4$ . Table I lists the numerically measured values  $\beta_m$ , obtained from the local slope  $d \ln S_m / d \ln t$ .

In general, the compound walk is confined to a certain ‘‘allowed’’ region of space. This region is bounded by multiple intersecting planes of the type  $x_i = x_j$  with  $i \neq j$ ,

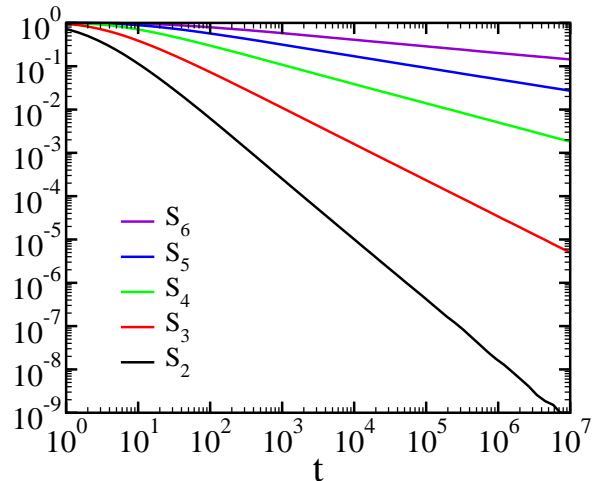


FIG. 4: The survival probability  $S_m(t)$  versus  $t$  for a four-particle system. Shown are the quantities  $S_2$  (bottom curve),  $S_3, \dots, S_6$  (top curve). The number of independent Monte Carlo runs varies from  $10^6$  for the slowest decay to  $10^{12}$  for the fastest decay.

and generally, this unbounded domain has a complicated geometry. The boundary of this region encloses a fraction  $V_m(N)$  of the total solid angle. On combinatorial grounds alone, we conveniently deduce that this fraction is given by the cumulative Mahonian distribution

$$V_m(N) = \sum_{l=0}^{m-1} P_l(N). \quad (19)$$

Since the Mahonian distribution is symmetric, we have  $V_m + V_{M+1-m} = 1$ . To evaluate  $V_m(N)$ , we expand the generating function (7), and for  $m \leq 4$ , we have [5]

$$V_m(N) = \frac{1}{N!} \times \begin{cases} 1 & m = 1, \\ N & m = 2, \\ \frac{1}{2}(N-1)(N+2) & m = 3, \\ \frac{1}{6}(N+1)(N^2+2N-6) & m = 4. \end{cases} \quad (20)$$

We have seen that the allowed region is a wedge when  $N = 3$ . To obtain an approximation for the first-passage exponents, we follow an approach that proved useful in other first-passage problems involving multiple random walks and replace the boundary of the allowed region with a suitably chosen cone in  $N-1$  dimensions [37]. An unbounded cone with opening angle  $\alpha$  occupies a fraction  $V(\alpha)$  of the total solid angle, given by

$$V(\alpha) = \frac{\int_0^\alpha d\theta (\sin \theta)^{N-3}}{\int_0^\pi d\theta (\sin \theta)^{N-3}}. \quad (21)$$

In  $d$  dimensions, we have  $d\Omega \propto (\sin \theta)^{d-2} d\theta$  where  $\Omega$  is the solid angle and  $\theta$  is the polar angle in spherical coordinates. In the cone approximation, we require

$$V(\alpha) = V_m \quad (22)$$

$m$	1	2	3	4	5	6
$V_m$	$\frac{1}{24}$	$\frac{1}{6}$	$\frac{3}{8}$	$\frac{5}{8}$	$\frac{5}{6}$	$\frac{23}{24}$
$\alpha_m$	0.41113	0.84106	1.31811	1.82347	2.30052	2.73045
$\beta_m^{\text{cone}}$	2.67100	1.17208	0.64975	0.39047	0.24517	0.14988
$\beta_m$	3	1.39	0.839	0.455	0.275	0.160

TABLE I: The six first-passage exponents for a four-particle system. The values  $\beta_m$  are from the Monte Carlo simulation results shown in Figure 4. The values  $\beta_m^{\text{cone}}$  were obtained using the cone approximation, specified in Eqs. (19)-(23). The cumulative Mahonian distribution,  $V_m$ , and the opening angle,  $\alpha_m$ , are listed as well.

with  $V_m$  given in (19).

In a cone, the first-passage exponent  $\beta \equiv \beta(\alpha)$  decreases as the opening angle  $\alpha$  increases. In particular,  $\beta = \pi/4\alpha$  in two dimensions, and  $\beta = (\pi - \alpha)/2\alpha$  in four dimensions. Generally, however,  $\beta$  is the smallest root of the following transcendental equation involving the associated Legendre functions [38] of degree  $2\beta + \gamma$  and order  $\gamma = \frac{N-4}{2}$  [17]

$$\begin{aligned} Q_{2\beta+\gamma}^\gamma(\cos \alpha) &= 0 & N \text{ odd,} \\ P_{2\beta+\gamma}^\gamma(\cos \alpha) &= 0 & N \text{ even.} \end{aligned} \quad (23)$$

Regardless of the dimension, the surface of a cone with  $\alpha = \pi/2$  is a plane, and hence,  $\beta(\pi/2) = 1/2$ .

For example, to find  $\beta_1(4)$ , we first determine the fraction  $V_1(4) = \frac{1}{4!} = \frac{1}{24}$  using (19). Then, we calculate the opening angle  $\alpha = 0.41113$  using equations (21)-(22) and finally determine the exponent  $\beta_1(4) = 2.67100$  as the appropriate root of equation (23). By construction, the cone approximation is exact for three particles. This approach gives a useful approximation to the six first-passage exponents when  $N = 4$  (Table I). Remarkably, the cone approximation continues to be a good approximation as the number of particles increases (Figure 5).

## VI. THE SCALING FUNCTION

We are especially interested in the behavior when the number of particles is large. Let us first evaluate the cumulative Mahonian distribution in the large- $N$  limit. Since the Mahonian distribution is normal, the cumulative distribution is given by the error function,

$$V_m(N) \rightarrow \frac{1}{2} + \frac{1}{2} \operatorname{erf}\left(\frac{z}{\sqrt{2}}\right), \quad (24)$$

when  $N \rightarrow \infty$ . Here,  $z$  is the scaling variable defined in (9) and  $\operatorname{erf}(\xi) = (2/\sqrt{\pi}) \int_0^\xi \exp(-u^2) du$ . To obtain Eq. (24), we substitute (10) into (19) and convert the sum into an integral. Equation (24) is relevant in the limit  $N \rightarrow \infty$ ,  $m \rightarrow \infty$  with the scaling variable  $z$  finite.

Next, we evaluate the solid angle enclosed by an unbounded cone when the dimension is large. The dominant contribution to the integral in (21) comes from a

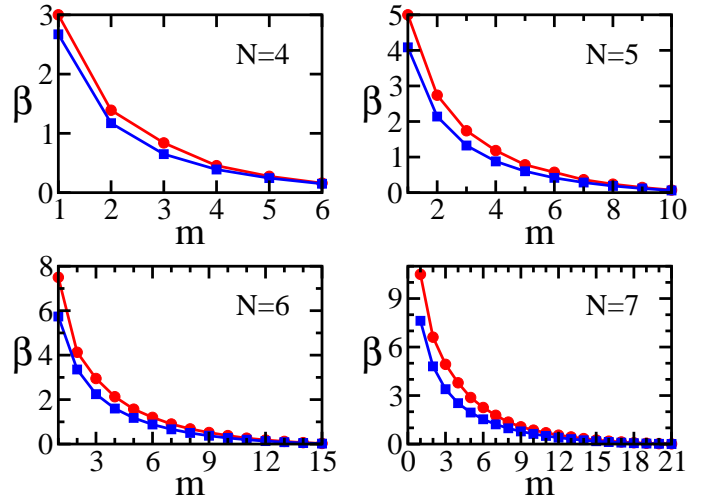


FIG. 5: The first-passage exponent  $\beta_m$  versus  $m$  for  $N = 4, 5, 6, 7$ . Shown are simulation results (circles) and the outcome of the cone approximation (squares).

narrow region of order  $1/\sqrt{N}$  centered on  $\alpha = \pi/2$  where the integrand is Gaussian,

$$(\sin \theta)^{N-2} \simeq e^{-N(\pi/2 - \theta)^2/2}.$$

Using  $\int_{-\infty}^{\infty} \exp[-N(\pi/2 - \theta)^2/2] d\theta \rightarrow \sqrt{2\pi/N}$ , we find that the fraction  $V(\alpha)$  has the scaling form

$$V(\alpha, N) \rightarrow \frac{1}{2} + \frac{1}{2} \operatorname{erf}\left(\frac{-y}{\sqrt{2}}\right), \quad (25)$$

with  $y = (\cos \alpha)\sqrt{N}$ . In writing this equation, we used the facts that  $\cos \alpha \simeq \pi/2 - \alpha$  and  $\operatorname{erf}(\xi) = -\operatorname{erf}(-\xi)$ . Equation (25) holds in the limit  $N \rightarrow \infty$ ,  $\alpha \rightarrow \pi/2$ , with the scaling variable  $y$  finite.

Asymptotic analysis of equation (23) shows that the exponent  $\beta(\alpha)$  adheres to the scaling form [17]

$$\beta(\alpha, N) \rightarrow \beta(y) \quad \text{with} \quad y = (\cos \alpha)\sqrt{N}, \quad (26)$$

in the limit  $N \rightarrow \infty$ ,  $\alpha \rightarrow \pi/2$  with the scaling variable  $y$  finite. The scaling function,  $\beta(y)$ , is specified by the transcendental equation  $D_{2\beta}(y) = 0$ , where  $D_\nu$  is the parabolic cylinder function of order  $\nu$  [38]. The smallest root is the appropriate one [17].

By comparing equations (24) and (25), we find our main result: the first-passage exponent depends on a single scaling variable,

$$\beta_m(N) \rightarrow \beta(z) \quad \text{with} \quad z = \frac{m - \langle m \rangle}{\sigma}, \quad (27)$$

in the large- $N$  limit. We reiterate that the average  $\langle m \rangle$  and the standard-deviation  $\sigma$  correspond to the steady-state values (4) and (8), respectively. Using  $y = -z$ , the scaling function  $\beta(z)$  is the smallest root of the transcendental equation

$$D_{2\beta}(-z) = 0, \quad (28)$$



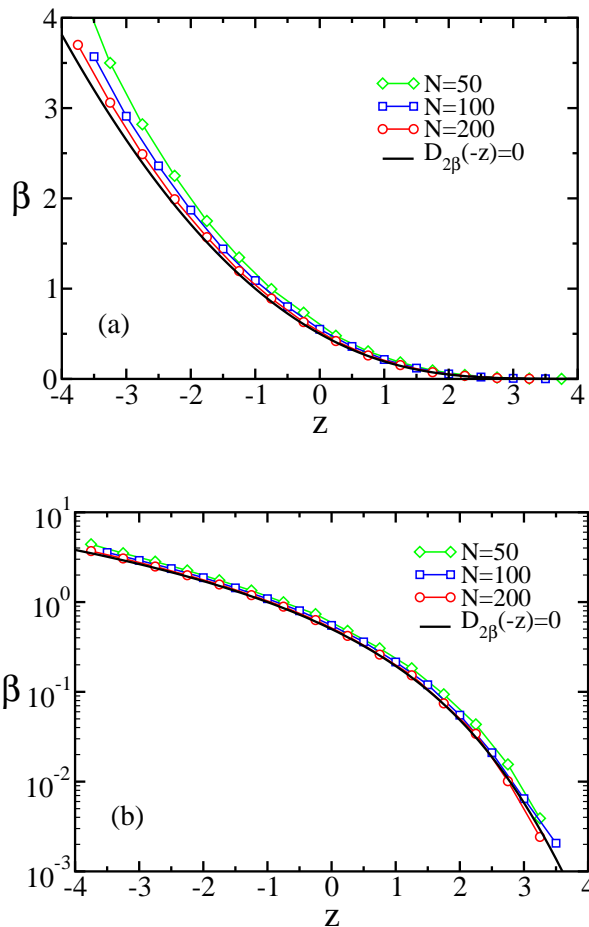


FIG. 6: The exponent  $\beta$  versus the scaling variable  $z$ , shown using: (a) a linear-linear plot and (b) a linear-log plot. The simulation results are from Monte Carlo runs with  $N = 50$  (diamonds),  $N = 100$  (squares), and  $N = 200$  (circles) particles. The number of independent realizations varies from  $10^4$  for slow first-passage processes to  $10^8$  for fast one. The solid line shows the theoretical prediction (28).

involving the parabolic cylinder function. When  $\beta$  is a half-integer, the parabolic cylinder function is related to the Hermite polynomials [38] and using this equivalence, we have  $\beta(0) = 1/2$ ,  $\beta(-1) = 1$ , and  $\beta(-\sqrt{3}) = 3/2$ .

Our numerical simulations (Figure 6) confirm that the exponents  $\beta_m(N)$  have the scaling form (27). Interestingly, the simulations strongly suggest that the scaling function predicted by the cone approximation is *exact*. We note that the convergence to the infinite-particle limit is very fast for positive  $z$ , but much slower for negative  $z$  [17].

With the power-law decay (17), the mean first-passage time diverges whenever  $\beta < 1$ , but it is finite otherwise. Since  $\beta(z = -1) = 1$ , the time required for the inversion number to reach one standard deviation from the mean is infinite, on average. Regardless of the threshold  $z$ , there is a considerable chance that the random walks are poorly mixed because the survival probability decays

$N$	3	4	5	6	7	8
$\beta_1$	$\frac{3}{2}$	3	5	$\frac{15}{2}$	$\frac{21}{2}$	14
$\beta_1^{\text{cone}}$	$\frac{3}{2}$	2.67100	4.08529	5.73796	7.62336	9.73686
$\beta_M^{\text{cone}}$	$\frac{3}{10}$	0.14988	0.061195	0.019895	0.0050713	0.0010266

TABLE II: The largest exponent,  $\beta_1^{\text{cone}}$ , and the smallest exponent,  $\beta_M^{\text{cone}}$ , obtained using the cone approximation for  $N \leq 8$ . Also listed for reference, is the exact value  $\beta_1$ .

algebraically.

The scaling behavior is remarkable for a number of reasons. First, the form of the scaling variable,  $z \equiv (m - N^2/4)/(N^{3/2}/6)$ , is quite unusual. Second, there are roughly  $N^2/2$  first-passage exponents and numerical evaluation of this large spectrum is daunting. Yet, the scaling form (27) gives the range of parameters for which  $\beta$  is of order one, and hence, numerically measurable. (It is difficult to measure a vanishing exponent,  $\beta \rightarrow 0$ , or a divergent exponent,  $\beta \rightarrow \infty$ .) Last, the emergence of scaling laws for a family of scaling exponents is also intriguing. Typically, in Statistical Physics, the opposite is true as one or two scaling exponents characterize a scaling law [39].

The extremal behaviors of the roots of the transcendental equation (28) are derived in ref. [17],

$$\beta(z) \sim \begin{cases} z^2/8 & z \rightarrow -\infty, \\ \sqrt{z^2/8\pi} \exp(-z^2/2) & z \rightarrow \infty. \end{cases} \quad (29)$$

The first-passage exponent is algebraically large if  $z$  is large and negative, but it is exponentially small if  $z$  is large and positive.

The exponential decay in (29) implies that it is extremely unlikely that the initial order is perfectly reversed. The smallest exponent  $\beta_M$  characterizes the probability  $S_M$  that the order of the walkers does not turn into the mirror image of the initial state, that is, the probability that the compound walk remains in the *exterior* of the so-called ‘‘Weyl chamber’’  $x_1 < x_2 < \dots < x_N$  [29–34]. This domain has  $V_M = 1 - \frac{1}{N!}$ , and Table II lists the outcome of the cone approximation for small  $N$ . To find the outcome of the cone approximation at large  $N$ , we first estimate the opening angle,  $\pi - \alpha \simeq e/N$  by using Eq. (21) and the Stirling formula  $N! \simeq \sqrt{2\pi N}(N/e)^N$ . From the asymptotic behavior for wide cones at large dimensions,  $\beta \simeq \sqrt{N/8\pi}(\pi - \alpha)^{N-3}$  [17], we conclude [37]

$$\beta_M \simeq \frac{N^4}{2e^3 N!}. \quad (30)$$

This value is extremely small, decaying roughly as the inverse of a factorial, and it is impossible to measure such a minuscule quantity using numerical simulations.

The largest exponent describes the probability that the particles maintain the initial order or that the compound walk remains in the *interior* of the Weyl chamber with  $V_1 = \frac{1}{N!}$ . Table II compares the outcome of the cone approximation with the exact value  $\beta_1 = N(N-1)/4$ . The

quality of the cone approximation worsens as  $N$  grows. Nevertheless, the cone approximation is qualitatively correct. By substituting the opening angle  $\alpha \simeq e/N$  into the thin-cone asymptotic behavior  $\beta(\alpha) \simeq N\alpha^{-1}/4$  [17], we find  $\beta_1 \simeq N^2/(4e)$ . This expression captures the quadratic growth of the exponent. Remarkably, the cone approximation is exact inside the scaling region, but it is only approximate outside this region.

## VII. CONCLUSIONS

In summary, we used the number of pair inversions to measure the one-dimensional mixing of independent diffusing trajectories. A high inversion number typifies strong mixing whereas a persistent small inversion number indicates poor mixing. In the steady-state, the distribution of inversion number is given by the well-known Mahonian distribution, and consequently, it is Gaussian when the number of particles is large. Preceding the steady-state is a transient regime in which both the average inversion number and the standard deviation grow diffusively with time.

We focused on first-passage statistics and showed that the probability that the inversion number does not exceed a certain threshold decays as power law with time. Moreover, we found that a large spectrum of decay exponents characterizes the asymptotic behavior. When the number of particles is large, the exponents obey a universal scaling function. The scaling variable equals the distance between the threshold inversion number and the average inversion number, measured in terms of the stan-

dard deviation.

The cone approximation, which replaces the region in which the compound random walk is allowed to move with an unbounded circular cone, plays a central role in our analysis. This approach is exact for three particles, it produces very good estimates in higher dimensions, and remarkably, this framework yields the exact scaling function. The cone approximation gives lower bounds for the decay exponents because, among all unbounded domains with the same solid angle, the perfectly circular cone maximizes the survival probability [37, 40, 41]. The cone approximation is useful in answering other first-passage questions such as the probability that the  $n$ th rightmost random walk does not cross the origin and the probability that the original rightmost particle always remains ahead of at least  $n$  other particles [37]. In both cases, there are as many exponents as there are particles, and curiously, the circular cone framework produces the scaling function governing the first-passage exponents approximately in the first case and exactly in the second case.

Understanding when the cone approximation is exact and when it is approximate is an interesting challenge, with implications well beyond first-passage [42–44]. The first-passage exponent is directly related to the lowest eigenvalue of the Laplace operator, and therefore, we conclude that the lowest eigenvalue of the Laplacian similarly obeys scaling laws in high dimensions. The shape of the scaling function depends on the actual geometry [45].

I thank Paul Krapivsky and Timothy Wallstrom for useful discussions. This research is supported by DOE grant DE-AC52-06NA25396.

- 
- [1] P. A. McMahon, *Amer. J. Math.* **35**, 281 (1913).
  - [2] W. Feller, *An Introduction to Probability Theory and Its Applications*, (Wiley, New York, 1968).
  - [3] G. E. Andrews, *The Theory of Partitions* (Addison-Wesley, Reading, 1976).
  - [4] M. Bóna, *Combinatorics of Permutations* (Chapman and Hall, Boca Raton, 2004).
  - [5] D. E. Knuth, *The Art of Computer Programming, vol. 3: Sorting and Searching* (Addison-Wesley, New York, 1998).
  - [6] J. Kleinberg and E. Tardos, *Algorithm Design* (Addison-Wesley, New York, 2005).
  - [7] J. M. Ottino, *Ann. Rev. Fluid Mech.* **22**, 207 (1990).
  - [8] G. A. Voth, G. Haller, and J. P. Gollub, *Phys. Rev. Lett.* **88**, (2002).
  - [9] J. M. Ottino and D. V. Khakhar, *Ann. Rev. Fluid Mech.* **32**, 55 (2000).
  - [10] S. B. Yuste and L. Acedo, *Phys. Rev. E* **64**, 061107 (2001); *Physica A* **297**, 321 (2001).
  - [11] S. B. Yuste, L. Acedo, and K. Lindenberg, *Phys. Rev. E* **64**, 052102 (2001).
  - [12] Q. H. Wei, C. Bechinger, and P. Leiderer, *Science* **287**, 625 (2000).
  - [13] B. X. Cui, H. Diamant, and B. H. Lin, *Phys. Rev. Lett.* **89**, 188302 (2002).
  - [14] S. Redner, *A Guide to First-Passage Processes* (Cambridge University Press, New York, 2001).
  - [15] R. D. DeBlassie, *Probab. Theory Relat. Fields* **74**, 1 (1987); *Probab. Theory Relat. Fields* **79**, 95 (1988).
  - [16] R. Bañuelos and R. G. Smiths, *Probab. Theory Relat. Fields* **108**, 299 (1997).
  - [17] E. Ben-Naim and P. L. Krapivsky, *Kinetics of First Passage in a Cone*, arXiv:1009.0238.
  - [18] G. H. Weiss, *Aspects and Applications of the Random Walk* (North-Holland, Amsterdam, 1994).
  - [19] H. C. Berg, *Random Walks in Biology* (Princeton University Press, Princeton, 1983).
  - [20] J. Rudnick and G. Gaspari, *Elements of the Random Walk: An Introduction for Advanced Students and Researchers* (Cambridge University Press, New York, 2004).
  - [21] B. Duplantier, in: *Einstein, 1905-2005*, eds. Th. Damour, O. Darrigol, B. Duplantier and V. Rivasseau (Birkhäuser Verlag, Basel, 2006); arXiv:0705.1951.
  - [22] R. E. Canfield, S. Janson, and D. Zeilberger, *The Mahonian Probability Distribution on Words is Asymptotically Normal*, *Adv. Appl. Math.*, in press (2010).
  - [23] P. L. Krapivsky, S. Redner, and E. Ben-Naim, *A Kinetic View of Statistical Physics* (Cambridge University Press,



- Cambridge, 2010).
- [24] T. E. Harris, *J. Appl. Prob.* **2**, 323 (1965).
  - [25] D. G. Levitt, *Phys. Rev. A* **6**, 3050 (1973).
  - [26] R. Arratia, *Ann. Probab.* **11**, 362 (1983).
  - [27] E. Barkai and R. Silbey, *Phys. Rev. Lett.* **102**, 050601 (2009).
  - [28] S. N. Majumdar, *Current Science* **77**, 370 (1999).
  - [29] M. E. Fisher, *J. Stat. Phys.* **34**, 667 (1984).
  - [30] D. A. Huse and M. E. Fisher, *Phys. Rev. B* **29**, 239 (1984).
  - [31] M. E. Fisher and M. P. Gelfand, *J. Stat. Phys.* **53**, 175 (1988).
  - [32] I. M. Gessel and D. Zeilberger, *Proc. Amer. Math. Soc.* **115**, 27 (1992).
  - [33] D. J. Grabiner, *Ann. Inst. Poincare: Prob. Stat.* **35**, 177 (1999).
  - [34] J. Cardy and M. Katori, *J. Phys. A* **36**, 609 (2003).
  - [35] F. Spitzer, *Trans. Amer. Math. Soc.*, **87** 187 (1958).
  - [36] D. ben-Avraham, B. M. Johnson, C. A. Monaco, P. L. Krapivsky, and S. Redner, *J. Phys. A* **36**, 1789 (2003).
  - [37] E. Ben-Naim and P. L. Krapivsky, First-Passage Exponents of Multiple Random Walks, arXiv:1009.02389.
  - [38] *NIST Handbook of Mathematical Functions*, ed. F. W. J. Olver, D. M. Lozier, et al. (Cambridge University Press, Cambridge, 2010).
  - [39] H. E. Stanley, *Introduction to Phase Transitions and Critical Phenomena* (Oxford University Press, New York, 1971).
  - [40] J. W. S. Rayleigh, *The Theory of Sound* (Macmillan, New York, 1877; reprinted Dover, New York, 1945).
  - [41] R. Courant and D. Hilbert, *Methods of Mathematical Physics*, vol. I (Wiley, New York, 1953).
  - [42] H. S. Carslaw and J. C. Jaeger, *Conduction of Heat in Solids* (Clarendon Press, Oxford, 1959).
  - [43] J. D. Jackson, *Classical Electrodynamics* (Wiley, New York, 1998).
  - [44] N. Th. Varopoulos, *Math. Proc. Camb. Phi. Soc.* **125**, 335 (1999); *Math. Proc. Camb. Phi. Soc.* **129**, 301 (1999).
  - [45] I. Chavel, *Eigenvalues in Riemannian geometry* (Academic Press, Orlando, 1984).